T. O. Rocheleau, T. Lin Naing, and C. T.-C. Nguyen, "*Long-Term Stability of a Hermetically Packaged MEMS Disk Oscillator*," *Proceedings*, 2013 IEEE International Frequency Control Symposium, Prague, Czech Republic, Jul. 22-25, 2013, pp. 209-212.

Long-Term Stability of a Hermetically Packaged MEMS Disk Oscillator

Tristan O. Rocheleau, Thura Lin Naing, and Clark T.-C. Nguyen
Dept. of Electrical Engineering and Computer Science
University of California, Berkeley
Berkeley, USA
Email: tristan@eecs.berkeley.edu

***Abstract*—A low phase noise oscillator referenced to a wine-glass disk MEMS resonator, hermetically vacuum packaged in a purpose-built packaging system, and measured in a double-oven, has provided a first long-term measurement of a MEMS disk oscillator over 10 months. After an initial burn-in period, the frequency can be seen to stabilize to within the short-term measurement variation of 300 ppb over a period of months, a significant improvement from previous studies on other MEMS resonator types, where frequency fluctuations were between 3.1 ppm and 1.2 ppm over similar time scales. Including burn-in, the total observed aging of 10 ppm is now on par with many consumer-grade quartz oscillators designed for timing applications and sufficient for target wireless sensor network applications.**

Keywords—MEMS oscillator, aging, long-term stability, hermetic packaging.

I. Introduction

MEMS-based resonators have emerged in recent years as low cost, on-chip alternatives to traditional quartz frequency references for use in timing applications [1]. Such devices offer not only valuable space savings in ever-shrinking consumer devices, such as cellular handsets, but also offer paths towards meeting the ultra-low-power requirements demanded by future wireless sensor networks [2]. While short-term stability of MEMS-based oscillators has proven to be quite good, where even the challenging GSM phase noise specifications were met some time ago [3], the long-term reliability and stability of such resonators has been largely unstudied.

Long-term frequency stability of reference oscillators is essential to maintain reliable radio communication without signals drifting into nearby bands. Typical frequency stability requirements are application-dependent and can range from tens of ppm per year to less than one ppm [4]. Cell phone requirements, for instance, remain one of the most challenging, with GSM requiring ±0.1 ppm reference oscillator stability [5]. Requirements for local-area wireless standards are much more lenient, however, with typical stability requirements of ±40 ppm [6]. Although the small size of MEMS resonators make them an exciting alternative to traditional quartz, they at the same time raise concerns of increased aging effects due to mass loading, package leaks, or stress fatiguing [7].

Some of the first published investigations on wafer-scale encapsulated resonators [8] indicated good stability, but measurements were of resonators only, not full oscillators, and were limited by experimental setup fluctuations to an accuracy of only ±3.1 ppm. Some more recent efforts have shown limited stability data of oscillators. One study [9] used an Aluminum-Nitride bulk acoustic wave resonator reference over 50 days of measurement. Here too, measurement setup fluctuations and lack of vacuum packaging, a necessary component for achieving the high Q of MEMS resonators, limited measurements to shorter time-scales and frequency fluctuations of ±1.2 ppm. Another study on a commercial device fabricated by SiTime [10] demonstrated exceptional short-term frequency stability of ±3 ppb, but only made measurements over periods of up to 15 minutes. Yet another study [11] demonstrated very close differential frequency tracking of two resonators over periods up to 30 days, but again intrinsic frequency stability was limited by measurement setup fluctuations.

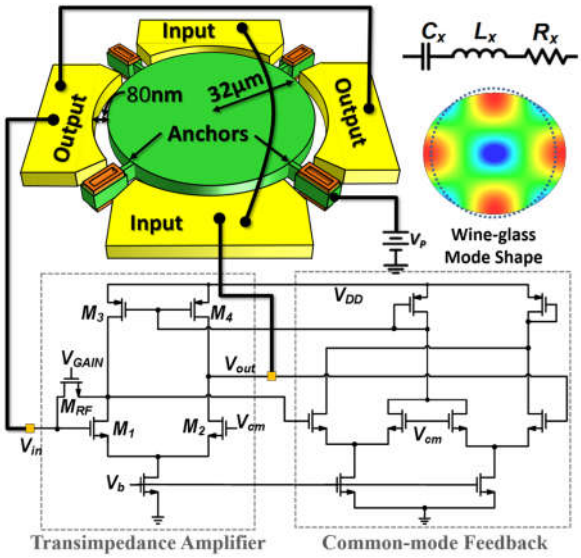

Fig. 1: Circuit schematic of the tested transimpedance amplifier-based micromechanical wine-glass disk oscillator, with the simplified equivalent circuit and mode shape for the MEMS resonator.

Meanwhile, wine-glass disk oscillators are known to exhibit exceptional short-term stability, with demonstrated phase noise below the GSM spec. [3] and superior insensitivity to vibration versus typical quartz counterparts [12]. But studies of long-term stability have until now been unpublished. To remedy this, this paper presents a first measurement of the MEMS oscillator of Fig.1, comprised of a wine-glass disk resonator bond-wired to

This work was supported in large part by the DARPA N/MEMS S&T program.

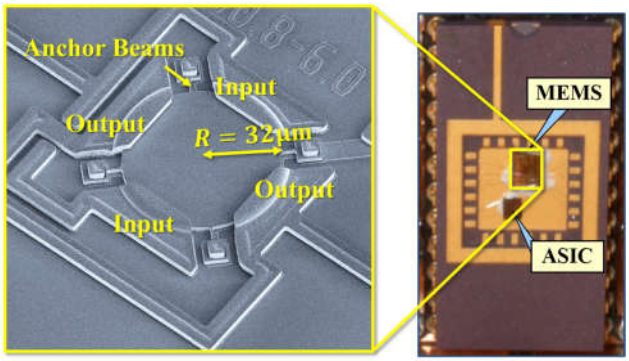

Fig. 2: SEM of the wine-glass disk resonator, left, bondwired into a DIP package with the ASIC amplifier, right.

an ASIC transimpedance amplifier and hermetically packaged in a custom-built vacuum-packaging system capable of maintaining μtorr pressures. A double-oven system maintains a constant oscillator temperature at 34°C with less than 0.001°C deviation, a key improvement over previous studies.

The long-term frequency drift of this MEMS oscillator is measured over 10 months and found to stabilize to within the short-term measurement variation of ±300 ppb over a period of months after an initial burn-in period. This marks a significant improvement from previous studies on other MEMS resonator types, where frequency fluctuations were ±3.1 ppm [8] and ±1.2 ppm [9] over similar time scales. Including burn-in, the total observed aging of 10 ppm over 10 months is now on par with many consumer quartz oscillators designed for timing applications [4] and marks performance sufficient for use in short range wirelesss sensor networks.

II. The MEMS Oscillator

The wine-glass disk resonator used in this work, cf. Fig. 2, was fabricated using the same process as [13] and consists of a 3μm-thick, polysilicon disk with 32μm-radius supported by four beams and surrounded by electrodes separated by a tiny 80 nm capacitive gap. The resonator motion is coupled to the electrical input and output via a bias voltage V_P applied to the disk. An ac drive voltage applied to the input electrode combines with V_P to produce a force across the input electrode-to-resonator gap that drives the resonator into the compound (2, 1) mode shape, shown in Fig. 1, which comprises expansion and contraction of the disk along orthogonal axes with nodal points located at support beam attachment locations. The relationship between the drive voltage and ensuing current generated by dc-biased mechanical modulation of the electrode-to-resonator gaps at each port is aptly modeled by the equivalent *LCR* circuit shown in Fig. 1. This mode's resonance frequency is given by:

$$f_{nom} = \frac{K}{R}\sqrt{\frac{E}{\rho(2+2\sigma)}} \qquad (1)$$

where R is the disk radius, $K = 0.373$ for polysilicon structural material, and E, σ, and ρ are Young's modulus, Poisson ratio, and density of the structural material, respectively.

To form an oscillator, the resonator is placed in the feedback path of a transimpedance amplifier similar to that of [12] and consisting of a fully differential CMOS amplifier connected in shunt-shunt feedback on one arm, with output taken from the other to realize a 0° phase shift from input to output. Transistors, M_1-M_4, comprise the basic differential pair biased by a common-mode feedback circuit that preserves low output resistance and cancels out common-mode noise. The MOS transistor M_{RF} is biased in the triode region to serve as a voltage controllable shunt-shunt feedback resistor that allows convenient adjustment of the TIA gain via its gate voltage, V_{GAIN}. When gain of the TIA is greater than the motional resistance of the resonator, R_x, the positive loop gain amplifies the (initially Brownian) motion until nonlinearity in either the amplifier or resonator (or both) limits the oscillation amplitude.

The amplifier IC was fabricated in a 0.35μm CMOS technology. Although the entire die occupies an area of 900μm×500μm, the actual sustaining amplifier only consumes about 100μm×100μm. The rest of the area is consumed by an on-chip buffer used to drive 50 Ω measurement systems and by-pass capacitors for noise reduction.

III. Stable Measurement Environment

A. Packaging

Of central import in MEMS oscillator stability is packaging. For example, exposure to air is known to produce frequency shifts due to oxidation or moisture absorption even in quartz oscillators [4]. The tiny size of MEMS resonators makes environmental control even more important. For the typical resonator used here, even a single additional monolayer of atoms, from sources such as contamination or package leakage, would correspond to a frequency change of over 30 ppm.

Beyond material aging concerns, a good vacuum environment is also needed to reduce air damping and enhance resonator Q. Fig. 3 gauges the degree to which air damping affects a typical wine-glass disk resonator used in this study with a measured plot of Q versus pressure that indicates a required operating pressure of below 1mtorr to remove air damping as a relevant loss mechanism. Achieving reliable hermetic packaging at such pressures is a challenge in a laboratory environment, and a chief obstacle in past long-term studies.

Pursuant to this goal, the vacuum packaging system of Fig. 4 was constructed to facilitate hermetic sealing using AuSn solder seals with a variety of conventional ceramic packages in a vacuum environment. In this system, a heated chuck holds the ceramic package containing the bond-wired MEMS resonator and ASIC while the package lid and magnetically attach to a linear motional feedthrough.

To package an oscillator, the ASIC and MEMS die, along

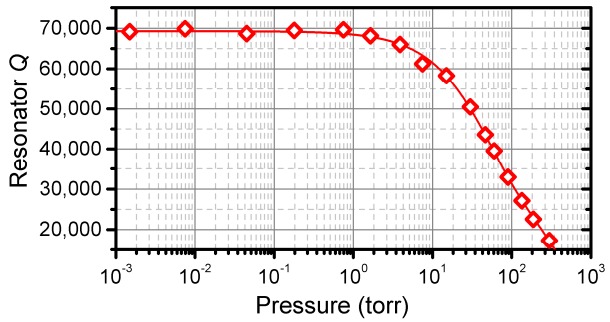

Fig. 3: Measured wine-glass disk MEMS resonator Q as a function of ambient air pressure.

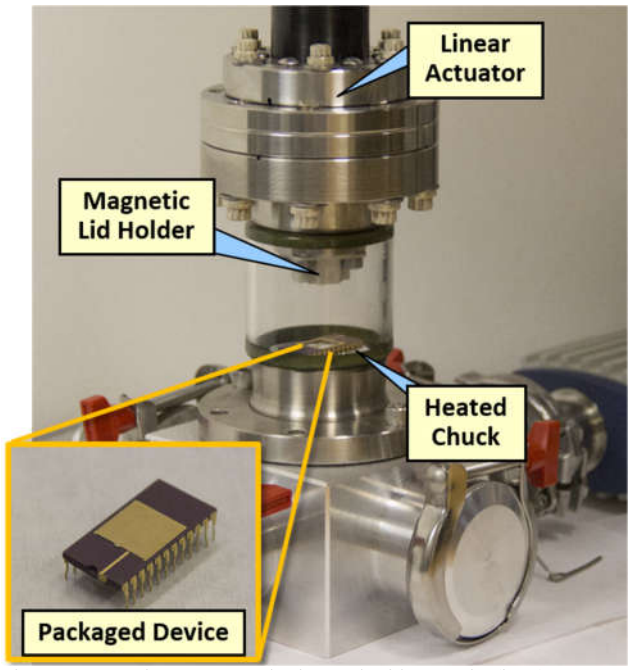

Fig.4: Hemermetic vacuum packaging tool with zoom-in (inset) on a DIP package sealed via the tool.

with Ti metal shavings used as a getter, are first glued within the package using Ceramabond 552 high-vacuum ceramic adhesive. The package is mounted in the packaging chamber and pumped to µtorr vacuum. Following a 2 hour bakeout at 220ºC, the package lid with AuSn preform is pressed with ~10 lbs. of force against the package and heated to 350ºC for 1 minute. The package and chuck are allowed to cool to room temperature before venting and unloading. For the oscillators in this study, Kyocera KD-78382-01 24-pin dual in-line packages (DIP) and HRC-2578 lids were used.

B. Temperature Control

In order to accurately measure true aging-induced frequency drifts, the oscillator temperature environment must be very tightly controlled or compensated. For the polysilicon devices used here, the measured temperature coefficient of frequency is on the order of $T_{CF} = 21$ ppm/°C, which allows excessive frequency shifts when ambient temperature fluctuations are not compensated. In the past, two methods of temperature compensation have been applied to MEMS oscillators. Passive compensation seems to be limited to ±40 ppm total frequency shift over commercial temperature ranges [9]. On the other hand, active temperature compensation is widely used in production MEMS oscillators to provide full temperature range stability to better than ± 10 ppm [14]. But to accurately observe true frequency drift in the absence of thermal variations, an even more stable temperature environment is needed.

To this end, the work presented here employs the double-oven setup of Fig. 5 to house the measured oscillators. The outer oven consists of a Cincinnati Sub-Zero MCB-1.2 chamber which keeps the internal temperature within ± 0.1C. To further stabilize temperature, a second internal oven combines a computer controlled heating element and temperature sensor incorporated into the box used to mount the oscillator. An ultra-

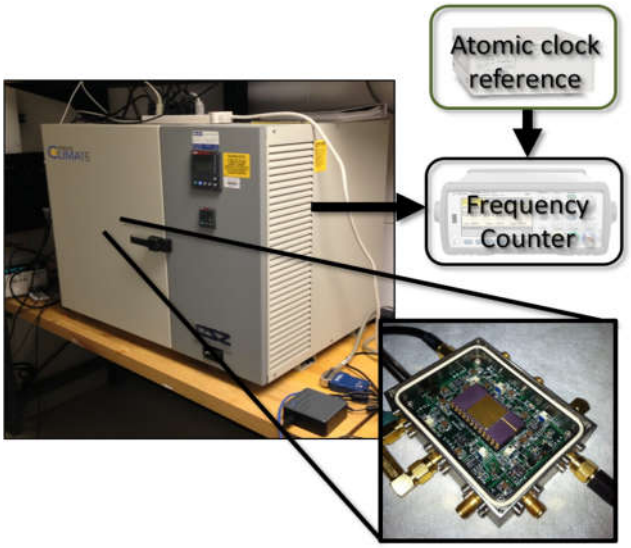

Fig.5: Experimental measurement setup showing the oscillator mounted in the first temperature controlled oven (inset) and placed in a second environmental chamber oven for further temperature stability. The oscillator frequency is measured via a zero dead-time counter referenced to an atomic clock.

stable Measurement-Specialties 46007 glass-encapsulated thermistor serves as the temperature monitor and control, measured using an Agilent 34420A micro-ohm meter. This double oven was observed to hold temperature to within ~200 µK in the face of typical daily external temperature fluctuations.

C. Frequency Measurement

When emplaced in the temperature-stable double-oven system, the oscillator output is measured using an Agilent 53230A frequency counter which allows high-resolution measurement with no dead time, i.e., no gap between measurements. For highly-stable measurements over long periods, a Stanford Research Systems FS725 atomic clock provides a frequency reference specified with ± 5 ppb aging over a 20 year lifespan.

IV. Measurement Results

Fig. 4 presents typical 1 day data for the oscillator mounted in the double-oven stabilization system and demonstrates remarkable frequency stability down to ±150 ppb. Fig. 7 presents measured oscillator frequency versus time data over a 10 month aging period, exhibiting the same logarithmic decay behavior typical of quartz oscillators [4]. The increasing frequency suggests possible stress relaxation or changes to the resonator material properties over mass loading or package leaks

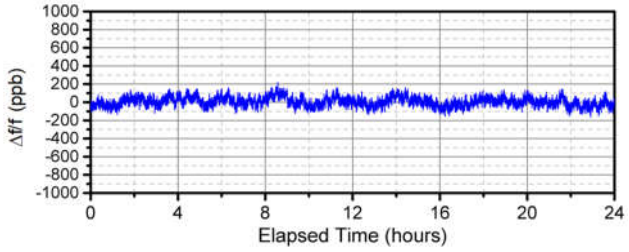

Fig. 4: Typical oscillator stability over 24 hours with a 1s averaging time.

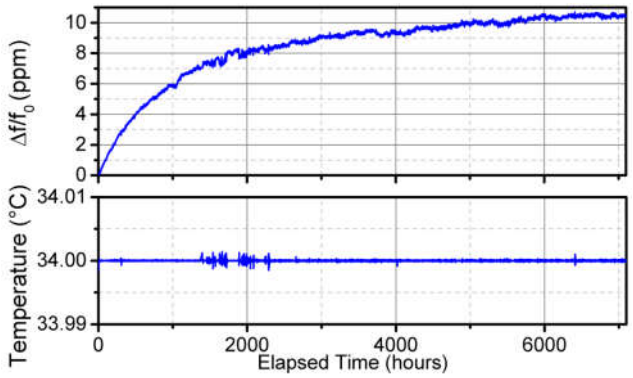

Fig. 7: Measured frequency drift and temperature stability of the MEMS oscillator. Frequency measurements were made using an Agilent 53230A frequency counter and shown here with a 100s measurement time.

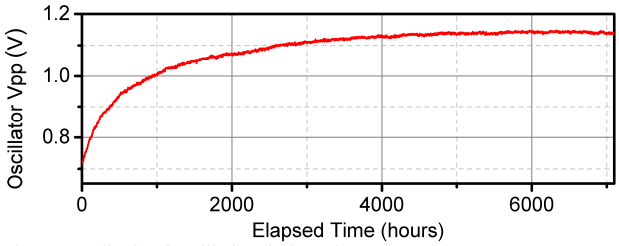

Fig. 8: Amplitude of oscillation during a long-term measurement.

as the aging mechanism. Stress relaxation in particular would be expected to contribute as both bond-wires and high-temp glue adhering the die to package would be expected to produce strain and have been observed to produce over 100 ppm/week drift in flexural mode devices [15]. Despite this, performance is good, on par even with low-cost quartz oscillators. This is not unexpected for such wine-glass devices, for which supports attached to quasi-nodal points on the resonant disk structure greatly isolate the disk from the substrate and its associated stress changes.

Interestingly, Fig. 8 presents oscillation amplitude data taken from this same time range, and shows an unexpected increase closely following the frequency drift seen. As the amplifier gain is kept fixed, this points to a surprising decrease in the R_x of the resonator over time. This again suggests that increased mass loading or air damping is not a factor here and further confirms a reliable package over the measured time span.

To better gauge the performance of this oscillator, Allan Deviation, σ_y, can be calculated from the fractional frequency shift $y_n = \Delta f / f_0$ using

$$\sigma_y^2(\tau) = \frac{1}{2}\langle(\bar{y}_{n+1} + \bar{y}_n)^2\rangle \qquad (2)$$

Fig. 9 presents Allan deviation vs. averaging time for the oscillator here. This plot closely follows typical performance of crystal oscillators [4], with decreasing Allan deviation for increasing measurement times up to approximately 1s as white phase and frequency noise are averaged out. Above 1s averaging time, the Allan deviations achieves a floor of $\sigma_y = 1.5\ x\ 10^{-8}$, competitive with typical quartz timing oscillators. As averaging time is increased, Allan Deviation remains constant till it begins to increase due to longer-term random walk noise, ultimately becoming dominated by long-term frequency drift effects.

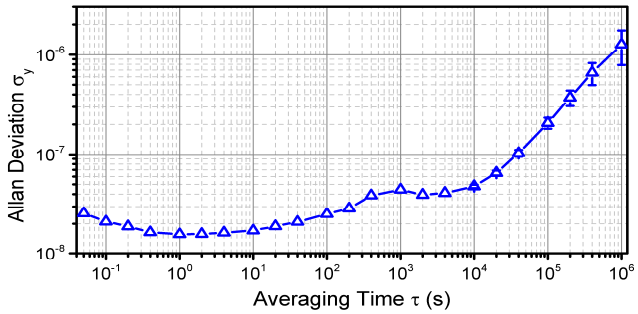

Fig. 9: Allan deviation as calculated from stability data with differing averaging times. Data with averaging time below 400s was calculated from shorter data sets taken at 0.01s sample time, while longer averaging time data was calculated from the full long-term stability data.

V. Conclusions

In this first study of long-term frequency drift in micromechanical wine-glass disk oscillators, performance is seen to be quite good, achieving stability within ± 300 ppb over a month after a burn-in period. With burn-in, the total drift is only 10 ppm over 10 months, well within required limits for many short-distance wireless communication specifications despite concerns that the small size of such MEMS resonators would lead to drift and reliability issues. Moreover, the increasing amplitude of oscillation over time suggests actual improvement in resonator quality factor and demonstrates that even simple in-house vacuum packaging is sufficient to achieve reliable operation of these MEMS devices. Whether or not Q's truly increase with time, the long-term stability measured here, together with the GSM-compliant phase noise already demonstrated in parallel work [3], elevates micromechanical wine-glass disk oscillators as some of the best MEMS has to offer, and encourages their use in small form factor, low power applications, such as the autonomous wireless sensor market, expected to grow exponentially in the coming years. More challenging cell phone reference oscillator requirements remain a target for future improvement.

References

[1] C. T. C. Nguyen, *UFFC Transactions,* vol. 54, pp. 251-270, 2007.
[2] J. M. Rabaey, J. Ammer, T. Karalar, L. Suetfei, B. Otis, M. Sheets, *et al.*, *ISSCC*, 2002, pp. 200-201 vol.1.
[3] Y.-W. Lin, S. Lee, S.-S. Li, Y. Xie, Z. Ren, and C.-C. Nguyen, *IEEE Journal of Solid-State Circuits,* vol. 39, pp. 2477-2491, 2004.
[4] J. R. Vig and T. R. Meeker, *Proceedings, FCS*, 1991, pp. 77-101.
[5] ETSI, Technical Specification 100 912
[6] IEEE, Standard 802.15.4
[7] C. L. Muhlstein, S. B. Brown, and R. O. Ritchie, *Journal of Microelectromechanical Systems,* vol. 10, pp. 593-600, 2001.
[8] B. Kim, R. N. Candler, M. A. Hopcroft, M. Agarwal, W.-T. Park, and T. W. Kenny, *Sensors and Actuators A,* vol. 136, pp. 125-131, 2007.
[9] R. Tabrizian, M. Pardo, and F. Ayazi, *Proceedings, IEEE Int. Conf. on MEMS*, 2012, pp. 23-26.
[10] L. Haechang, A. Partridge, and F. Assaderaghi, *Frequency Control Symposium*, 2012, pp. 1-5.
[11] E. J. Ng, L. Hyung Kyu, A. Chae Hyuck, R. Melamud, and T. W. Kenny, *IEEE Sensors Journal,* vol. 13, pp. 987-993, 2013.
[12] T. L. Naing, T. O. Rocheleau, R. Zeying, E. Alon, and C. T. C. Nguyen, *Proceedings, FCS*, 2012, pp. 1-6.
[13] M. A. Abdelmoneum, M. U. Demirci, and C. T. C. Nguyen, *Proceedings, IEEE Int. Conf. on MEMS*, 2003, pp. 698-701.
[14] Discera Corporation, "DSC1121 Datasheet."
[15] V. Kaajakari, J. Kiihamaki, A. Oja, H. Seppa, S. Pietikainen, V. Kokkala, *et al.*, *Proceedings, TRANSDUCERS*, 2005, pp. 916-919 Vol. 1.